Theoretical Study of the Optical Manipulation of Semiconductor Nanoparticles under an Excitonic Resonance Condition

Takuya Iida and Hajime Ishihara*

Department of Physical Science, Graduate School of Engineering Science, Osaka University, Toyonaka, Osaka 560-8531, Japan

(Received 19 December 2001; published 5 February 2003)

We theoretically study the mechanical interaction between radiation and a semiconductor nanoparticle, based on a microscopic model of confined excitons. The exerted force is calculated by using the Maxwell stress tensor expressed in terms of the microscopic response field. The numerical demonstrations clarify the following: (1) The enhancement of the force by using electronic resonance is remarkable for a particle with a radius of less than 100 nm for semiconductor materials. (2) The spectral peak position of the exerted force is considerably sensitive to nanoscale-size changes which would be useful for highly accurate size-selective manipulation.

DOI: 10.1103/PhysRevLett.90.057403 PACS numbers: 78.67.Bf, 71.35.–y, 78.90.+t

Since the trapping of dielectric particles was demonstrated by Ashkin *et al.* in 1986 [1] through the use of radiation pressure, this optical-tweezers technique has been developed and is now widely applied in a variety of fields to manipulate micron-size objects [2]. One of the current interests in this field is the use of radiation force to manipulate smaller (nanoscale) objects effectively. For metallic substances, the trapping of a particle with a diameter of 40 nm has been demonstrated [3]. For nonmetallic substances, it has been reported that organic molecules with sizes in the hundreds of nm can be gathered by a strongly focused laser beam [4]. As for theoretical studies, methods that use strongly localized evanescent fields have been proposed for the manipulation of nanoparticles [5,6], where the steep gradient of field intensity generates a strong dipole (gradient) force. For the usual dielectric particles larger than light wavelength, the exerted force is enhanced by the Mie resonance (due to the background dielectric constant) where light is strongly scattered and the momentum of light is efficiently transferred to the matter. However, if the particle is much smaller than the wavelength for the usual laser frequency region, the Mie resonance frequencies go beyond this frequency region. Hence it is difficult to exert a strong enough force on nanoscale objects in the available frequency region. On the other hand, it is well known that induced polarization is generally enhanced when the incident light is resonant with an electronic transition energy of matter; this enhancement, in turn, increases either scattering or the gradient force. As this mechanism is used in the atom-trapping technique [7], the resonance condition is expected to significantly enhance exerted force even on nanoscale objects. Although resonant excitation usually causes a heating problem in condensed matter because of the nonradiative decay of the excitation, this problem can be avoided if the electronic systems confined in the objects have good coherence, so that the radiation-matter coupling is much larger than the nonradiative decay constant. In such a case, the induced force is dominated by coherent scattering with less absorption. Moreover, it will be possible that objects of particular sizes or shapes can be mechanically separated by using a resonant light, because the resonance condition sensitively depends on such properties of individual nanoscale objects. In order to demonstrate the possibility of such a new type of optical manipulation linked to the quantum properties of nanoscale objects, we study the radiation-matter mechanical interaction under the resonance condition based on the quantum mechanical treatment of the matter system. No such study has been explicitly done in the previous works that have treated the nonresonance condition [8–11].

The optical response of a confined electronic system depends strongly, in general, on the system's geometrical properties, in particular, the size quantization and the nanoscale spatial structures of the response internal fields [12]. Such features should be reflected in the characteristics of the exerted force through their size and frequency dependence, which should be derived from the microscopic model of the matter. According to standard electromagnetics, the exerted force on a substance in the presence of electric and magnetic fields ($\mathbf{E}$ and $\mathbf{H}$) satisfying the Maxwell equations (namely, the Maxwell fields) can be expressed by the integration of the Maxwell stress tensor over the surface around the object as $\langle \mathbf{F} \rangle = \langle \int_S \mathbf{T} \cdot \mathbf{n} dS \rangle$ [13], where $\langle\rangle$ is the time average, $\mathbf{n}$ is a normal vector at the surface surrounding the object, $\mathbf{T}$ is a stress tensor, i.e., $\mathbf{T} = \mathbf{EE} + \mathbf{HH} - (1/2)(|\mathbf{E}|^2 + |\mathbf{H}|^2)\mathbf{I}$, and $\mathbf{I}$ is a unit tensor. Since this relation can be derived regardless of whether the fields are macroscopic or microscopic, we can calculate the exerted force reflecting the quantum structure of the nano-objects using microscopic fields in the above expression of $\langle \mathbf{F} \rangle$. Therefore, in the first step, we calculate the microscopic Maxwell fields by solving the Maxwell equations that contain the dielectric function calculated from the quantum mechanical model of nano-objects.

As a typical example of electronic excited states, we consider the excitons confined in a nanosphere. Assuming that the Bohr radius of the relative motion of an electron and a hole is much smaller than the sphere, we explicitly treat only the degree of freedom of the center-of-mass (c.m.) motion. The eigenenergy of the bulk exciton generally has the wave number (k) dependence because of the c.m. motion, as $E(k) = \hbar\omega_T + \hbar^2k^2/2M_{\rm ex}$, where $\hbar\omega_T$ is the energy of the bulk transverse exciton and $M_{\rm ex}$ is its translational mass. Therefore, the dielectric function arising from the exciton has spatial dispersion (or k dependence), which is written as

$$\varepsilon(\omega, k) = \varepsilon_b + \frac{\varepsilon_b \Delta_{LT}}{\hbar\omega_T + \hbar^2k^2/2M_{\rm ex} - \hbar\omega - i\Gamma}, \qquad (1)$$

where ε_b is the background dielectric constant and Δ_{LT} is the splitting between $\hbar\omega_T$ and the longitudinal exciton energy ($\hbar\omega_L$). In order to obtain the response to a given incident field, we need to connect the solutions of the Maxwell equations inside and outside the sphere. Since the dispersion relation $(\omega^2/c^2)\varepsilon(\omega, k) = k^2$ in the sphere yields two different wave numbers in general, the usual Maxwell boundary conditions are not sufficient for the unique connection. It has been well discussed that this problem can be managed by introducing the boundary conditions for the excitonic polarizations at the surface [14,15], i.e., the additional boundary conditions (ABCs). Following Ref. [16], we use the Pekar-type ABCs, which require the excitonic polarizations to vanish at the surface. This is equivalent to considering the nonescape boundary condition for the c.m. wave functions of the exciton [15].

In the following calculations, we consider the two types of incident fields, i.e., the propagating plane wave $\mathbf{E}^i_+(z)$ and the standing plane wave $\mathbf{E}^i_+(z) + \mathbf{E}^i_-(z)$, where $\mathbf{E}^i_\pm(z) = E_0\{0, \exp[\pm ik_0(z - z_1)], 0\}\exp[-i\omega t]$ and k_0 is the wave number in a vacuum. In the former case, both the scattering and the absorbing forces are dominantly induced, while the gradient force (dipole force) is dominantly induced in the latter case. We expand these fields with the spherical surface harmonics, assuming the center of the particle is located at $z = 0$, and perform the procedure explained above to derive the response field. The obtained response field is used in the calculation of the Maxwell stress tensor in $\langle\mathbf{F}\rangle$. For the numerical demonstration, the incident intensity is assumed to be 50 μW/100 μm^2 [$|E_0|^2 = 12\pi \times 10^7$(V^2/m^2)], which is within the linear response regime [17].

First, we study the merit of using electronic resonance to enhance the force on nanoscale objects, considering a CuCl particle irradiated by the propagating plane wave field resonant with a Z_3 exciton that is a typical single-component Wannier-type exciton. [The parameters are $\epsilon_b = 5.59$, $\hbar\omega_T = 3.2022$(eV), $\Delta_{LT} = 5.7$(meV), and $M_{\rm ex} = 2.3m_0$, where m_0 is the free electron mass.] The nonradiative decay constant is assumed to be 20 μeV [17]. For a 100 nm radius, no significant difference can be found between the maximum value of the force enhanced by the Mie resonance and that enhanced by the excitonic resonance [Fig. 1(a)]. However, as the radius becomes smaller, the peaks of the Mie resonance move to the higher-energy region, and the exerted force due to the scattering by the background dielectric constant alone becomes very small in the available frequency region. On the other hand, the exerted force due to the excitonic resonance is greatly enhanced as compared to the force in the nonresonant case [Fig. 1(b)].

For an even smaller particle, the difference becomes much more significant. In contrast with the enhanced force due to the excitonic resonance, the force in the absence of the resonance becomes negligibly small, and its spectrum is structureless in the usual laser frequency region [see Fig. 2(c) for 10 nm radius]. Converting the force into the acceleration, we show the size dependence of its maximum value in the energy range $0 \sim 4.0$ eV together with the gravitational acceleration in Fig. 1(c). For a 10 nm radius, for example, the acceleration near the excitonic resonance is almost 10^4 times larger than that in the absence of resonance. (We obtain a similar result for the parameters of ZnO A-exciton.) Thus, there is clearly merit in using electronic resonance for the optical manipulation of nanoscale particles.

Next, we observe the spectral structure of the induced force near the excitonic resonance and then discuss the peak specific feature of the force. Figure 2(a) shows the fine structures near the excitonic resonance for a 50 nm radius, where several peaks appear between $\hbar\omega_T$ and $\hbar\omega_L$ (3.2079 eV) reflecting the size-quantized c.m. levels.

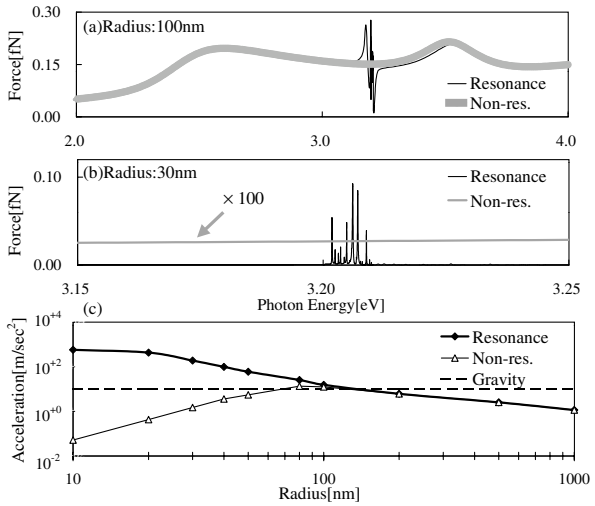

FIG. 1. (a),(b) Frequency dependence of the radiation force. (c) Size dependence of the maximum value of the acceleration induced by radiation force in 0–4 eV. In (a)–(c), "Non-res." means the results in the absence of the resonance term in Eq. (1). In (c), the gravitational acceleration is also shown.

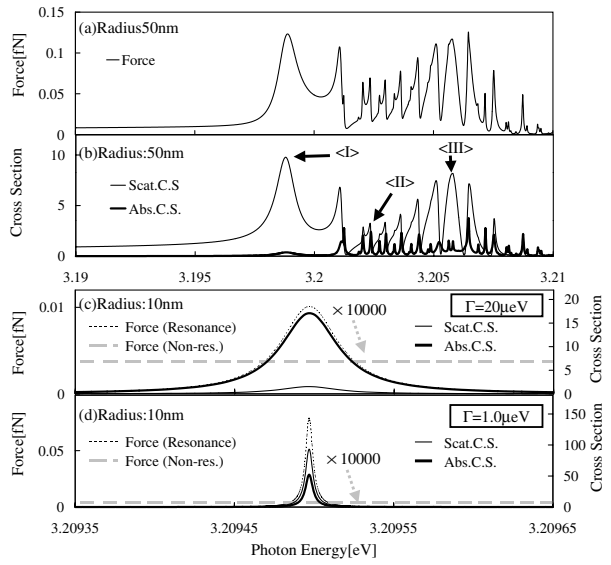

FIG. 2. (a) Frequency dependence of the radiation force. (b) The scattering and absorption cross sections (normalized by πR^2). (c),(d) Frequency dependence of the radiation force near the peak of the second-lowest level of the TM mode exciton (the most prominent one in the spectrum). The scattering and absorption cross sections are shown together.

Here, we should note that the character of the force drastically changes with the frequency. For example, as shown in Fig. 2(b), the absorption cross section $\sigma_{\rm abs}$ is very small compared with the scattering cross section $\sigma_{\rm sc}$ around the peak below the lowest (TE mode) excitonic level (indicated by the arrow $\langle$I$\rangle$) and those just below $\hbar\omega_L$ (indicated by the arrow $\langle$III$\rangle$), where the weight of the absorbing force is much smaller than that of the scattering force. In the former region, this is because the (size-dependent) radiation-exciton coupling is much larger than the assumed nonradiative decay constant, which means the radiative decay is much faster than the nonradiative one. In the latter region, radiation-exciton coupled modes (polaritons) have a surface mode nature with less absorption. On the other hand, within the region between $\hbar\omega_T$ and $\hbar\omega_L$, $\sigma_{\rm abs}/\sigma_{\rm sc}$ is relatively large, where the absorbing force is heavier. [See the arrow $\langle$II$\rangle$ in Fig. 2(b).] In the case of the resonant excitation, the absorption is usually so large that the heating problem becomes serious for optical manipulation. However, under the condition that the radiative decay is much faster than the nonradiative one (which occurs around the energy indicated by the arrow $\langle$I$\rangle$), the force is dominated by the elastic light scattering, and heating can be reduced even in the resonance condition. Such a condition is peculiar to confined systems in nanostructures where the well-maintained coherency of some excited states causes the large radiation-matter coupling. For a smaller particle (with a 10 nm radius), $\sigma_{\rm abs}$ becomes much larger than $\sigma_{\rm sc}$ for $\Gamma = 20$ μeV, because the radiative coupling of the exciton is smaller than the nonradiative decay constant in this condition [Fig. 2(c)]. However, if Γ is rather small, as reported for the CuCl nanocrystals (1 μeV) [18], $\sigma_{\rm sc}$ exceeds $\sigma_{\rm abs}$, and thus the scattering force becomes dominant even in such a small particle [Fig. 2(d)].

The peak specific feature of the force is related to the nanoscale spatial structures of the internal field. In Fig. 3, the absolute values of the field amplitude are plotted as functions of the position in the xz plane for $y = 0$ at the peak positions corresponding to $\langle$I$\rangle$–$\langle$III$\rangle$. At the peak $\langle$I$\rangle$, the spatial structure reflecting the excitonic state with the p-orbital character (angular momentum $l = 1$) appears [Fig. 3(b)]. Such a whispering gallery mode-like structure arises even for a very small particle because of the coherent interaction between the radiation and exciton (polaritonic effect), which leads to an enhancement of the exerted force with less absorption. Figures 3(c) and 3(d) refer, respectively, to the peak at which the absorption component is relatively large [$\langle$II$\rangle$ in Fig. 2(b)] and the peak slightly below $\hbar\omega_L$, where the scattered component is larger [$\langle$III$\rangle$ in Fig. 2(b)]. In the former, the internal field is strong at the core of the particle, whereas in the latter, the field is strong near the surface, reflecting the surface mode nature.

Finally, we show the force spectrum in the case of the standing plane wave. In this case, we consider $\mathbf{E}^i_+(z) + \mathbf{E}^i_-(z)$ as an incident wave, and we analytically obtain the relation $\langle F_z\rangle \propto |E_0|^2\, 4k_0 \sin(2k_0 z_1) = \nabla_z |\mathbf{E}^i_+(z) + \mathbf{E}^i_-(z)|^2_{z=0}$. This indicates that the exerted force is the gradient one, which peaks when $z_1 = \pm(\lambda/8 + n\lambda/2)$, $(n = 1, 2, \ldots)$, where λ is the wavelength of light in a vacuum. Figure 4(b) shows the exerted force when $z_1 = -\lambda/8$. As discussed before [7], the direction of the gradient force changes at the resonance poles. It should be remarked that such poles generally include the radiative shift. In the present case, the direction of the

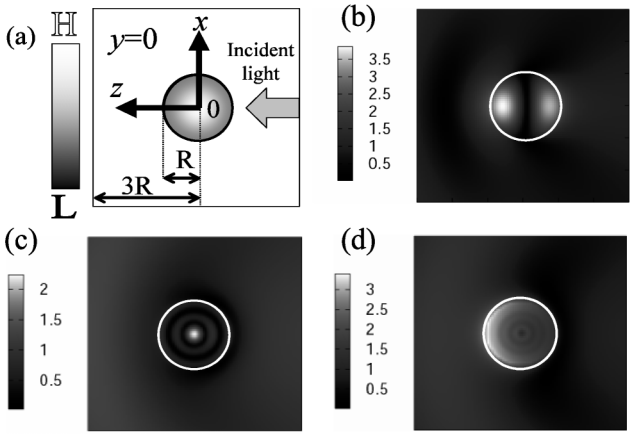

FIG. 3. The spatial distribution of the absolute value of the electric field for a 50 nm radius. The direction of polarization is normal to the xz plane. A particle occupies the inside of the white circle in each figure. (a) The considered geometry. (b) $\hbar\omega = 3.199$ (eV). (c) $\hbar\omega = 3.2023$ (eV). (d) $\hbar\omega = 3.2057$ (eV).

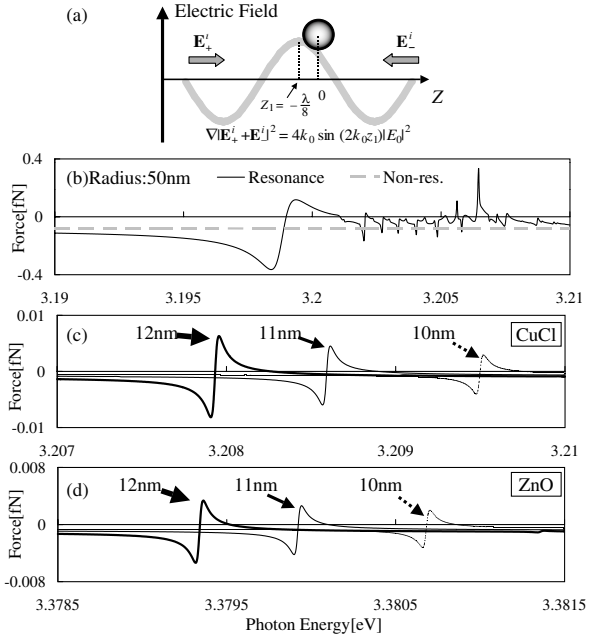

FIG. 4. The force spectra in the case where a particle is irradiated by a standing wave field. The considered geometry is explained in (a). The parameter values for ZnO are $\epsilon_b = 4.0$, $\hbar\omega_T = 3.375\,25$ (eV), $\Delta_{LT} = 2.16$ (meV), $M_{\rm ex} = 0.87m_0$, $\Gamma = 20$ (μeV).

force due to the lowest (TE mode) excitonic resonance changes rather far from the bare excitonic level because of the large radiative shift which, in turn, is due to the coherent extension of the c.m. wave function.

The characteristic behavior of the gradient force appears in a clearer way in the smaller case because the separation between the quantized levels is larger. Figures 4(c) and 4(d) show the force spectrum for several radii of around 10 nm for CuCl and ZnO. A particularly noteworthy point is that the peak position is very sensitive to the change in the size of the nanometer order. In the present case, the exerted force on the particle is directed to the antinode (node) position of the field below (above) the resonance energy. This mechanism would be useful for accurate size-selective optical manipulation and fabrication of resonant photonic crystals.

In conclusion, our theoretical demonstration shows significant merit in the use of electronic resonance for the optical manipulation of particles of less than 100 nm radius. For smaller particles (around 10 nm radius), the exerted force near the resonance can be especially enhanced — as much as 4 or 5 orders of magnitude larger than that in the absence of the resonance. Furthermore, it should be remarked that there are conditions where radiation-matter coupling is much larger than the usual nonradiative damping constant for the confined excitons in nanoscale objects. In such conditions, the scattering force is much heavier than the absorbing one, which is favorable for optical manipulation under the resonance condition. One of the attractive points of optical manipulation using a resonant light is that it can mechanically separate particular objects from others because the force spectrum of confined systems sensitively depends on the properties of individual objects, such as the size and shape. The nanoscale-size selection is such an example. Although our theoretical demonstration is done only for a plane wave field by considering a simple environment, the above results are encouraging for similar studies in the cases of evanescent and focused fields, and for more realistic situations with respect to the environments of the objects.

The authors are grateful to Professor K. Cho for the fruitful discussions and support. They also thank Dr. H. Ajiki and Mr. K. Kawano for their useful discussions. This work was supported in part by grants-in-aid for Scientific Research (10207205) and for COE Research (10CE2004) from the Ministry of Education, Science, Sports and Culture of Japan.

*Electronic address: ishi@mp.es.osaka-u.ac.jp

[1] A. Ashkin, J. M. Dziedzic, J. E. Bjorkholm, and S. Chu, Opt. Lett. **11**, 288 (1986).
[2] See articles in *Forces in Scanning Probe Methods*, edited by H.-J. Guntherodt, D. Anselmetti, and E. Meyer, NATO ASI Series (Kluwer Academic Publishers, Dordrecht, 1995).
[3] T. Sugiura, T. Okada, Y. Inouye, O. Nakamura, and S. Kawata, Opt. Lett. **22**, 1663 (1997).
[4] S. Ito, H. Yoshikawa, and H. Masuhara, Appl. Phys. Lett. **78**, 2566 (2001).
[5] L. Novotny, R. X. Bian, and X. S. Xie, Phys. Rev. Lett. **79**, 645 (1997).
[6] K. Okamoto and S. Kawata, Phys. Rev. Lett. **83**, 4534 (1999).
[7] C. Cohen-Tanoudji, in *Fundamental Systems in Quantum Optics*, Proceedings of the Les Houches Summer School, Session LIII, edited by J. Dalibard, J. Raimond, and J. Zinn-Justion (North-Holland, Amsterdam, 1992).
[8] J. P. Barton, D. R. Alexander, and S. A. Schaub, J. Appl. Phys. **66**, 4549 (1989).
[9] A. Ashkin, Biophys. J. **61**, 569 (1992).
[10] T. Sugiura and S. Kawata, Bioimaging **1**, 1 (1993).
[11] P. C. Chaumet and M. Nieto-Vesperinas, Phys. Rev. B **61**, 14 119 (2000); **62**, 11 185 (2000).
[12] H. Ishihara, K. Cho, K. Akiyama, N. Tomita, Y. Nomura, and T. Isu, Phys. Rev. Lett. **89**, 017402 (2002).
[13] J. D. Jackson, *Classical Electrodynamics* (Wiley, New York, 1999), 3rd ed.
[14] S. I. Pekar, Sov. Phys. JETP **6**, 785 (1957).
[15] L. Birman, in *Excitons*, edited by E. I. Rashba and M. D. Sturge (North- Holland, Amsterdam, 1982), p. 27.
[16] R. Ruppin, J. Phys. Chem. Solids **50**, 877 (1989).
[17] T. Mita and N. Nagasawa, Solid State Commun. **44**, 1003 (1982).
[18] M. Ikezawa and Y. Masumoto, Phys. Rev. B**61**, 12 662 (2000).